Effect of Foehn Wind on Record-Breaking High Temperature Event (41.1°C) at Kumagaya on 23 July 2018

Akifumi Nishi[1] and Hiroyuki Kusaka[2]
[1]*Graduate School of Life and Environmental Sciences, University of Tsukuba, Tsukuba, Japan*
[2]*Center for Computational Sciences, University of Tsukuba, Tsukuba, Japan*

Abstract

In this study, we use observational data and numerical models to reveal whether foehn wind affects the record-breaking high-temperature event (41.1°C) at Kumagaya on July 23, 2018. On this day, the weather conditions at Kumagaya satisfied the conditions described in Takane et al. (2014) for a likely extreme high temperature (EHT) day: a "whale-tail" pressure pattern, no precipitation for 6 days, a high potential temperature at 850 hPa, and northerly surface winds. Our back-trajectory analysis shows that the air parcels came to Kumagaya from heights up to 3.0 km above sea level over the Sea of Japan. The Lagrangian energy budget analysis shows that adiabatic heating accounts for about 87.5% of the increase of the thermal energy given to the air parcel, with the rest from diabatic heating. The diabatic heating is caused by heating associated with surface sensible heat flux and the mixing by turbulent diffusion. The adiabatic and diabatic heating are calculated to have raised the temperature of air parcel by 14 and 2.0 K, respectively, for this EHT event. We conclude that the dynamic foehn effect and diabatic heating from the surface, together with mixing in the atmospheric boundary layer, affected the formation of this EHT event.

(**Citation**: Nishi, A., and H. Kusaka, 2018: Effect of foehn wind on record-breaking high temperature event (41.1°C) at Kumagaya on 23 July 2018. *SOLA*, **15**, 17−21, doi:10.2151/sola.2019-004.)

1. Introduction

An extreme high-temperature (EHT) event brings widespread public-health risks such as heatstroke and sleep disturbance. Such an event also increases energy demand in urban areas.

Over the last decade, Japan has experienced record-breaking high temperatures of 40.9°C at Kumagaya and Tajimi on 16 August 2007, and of 41.0°C at Ekawasaki on 12 August 2013. Kumagaya lies in the Kanto Plain, an area that includes the Tokyo metropolitan area (K in Fig. 1a). The plain is bounded by the Pacific Ocean on the south and east sides, whereas the inland region is bound by the Chubu Mountains on north and west sides. This inland region is well-known for experiencing EHT events. Here, the frequency of EHT events and the daily maximum temperature have been increasing over the past few decades (e.g., Fujibe 1995). These increases are often attributed to global warming and the urban heat island effect. Takane et al. (2014) identified four conditions for an EHT event at Kumagaya: (1) High temperature at 850 hPa, (2) Synoptic pressure pattern is a "whale-tail pattern" of which pressure ridge expands westward from the northwest Pacific Ocean to the Yellow Sea, (3) a northwest surface wind, and (4) clear-sky days for 4 days or more.

The foehn is a downslope wind that is warm and very dry (e.g., Brinkmann 1971; WMO 1992). According to Elvidge and Renfrew (2016), foehns come in four types according to the dominant heating mechanism: (a) isentropic drawdown, in which the foehn air comes from higher, potentially warmer and dryer altitudes upwind of the mountain barrier due to the blocking of low-level flow by the mountain (type-a foehn wind) (Ficker 1910; Scorer and Klieforth 1959; Arakawa 1969; Brinkmann 1973, 1974; Ikawa and Nagasawa 1989; Seibert 1990; Richner and Hächler 2013), (b) precipitation and latent heating, in which cooling during uplift on the windward slopes promotes condensation, cloud formation, and subsequently precipitation leading to moisture removal and irreversible latent heating (type-b foehn wind) (Hann 1866, 1867; Barry 1992; Whiteman 2000; Richner and Hächler 2013), (c) turbulent sensible heating and drying of the low-level flow via mechanical mixing above rough, mountainous terrain in a stably stratified atmosphere (type-c foehn wind) (Scorer 1978; Ólafsson 2005), (d) radiative heating of the low-level lee side due to the dry, cloud-free foehn conditions (type-d foehn wind) (Hoinka 1985; Ólafsson 2005). Recent studies have also argued for combined foehn mechanisms (Takane and Kusaka 2011; Takane et al. 2015; Miltenberger et al. 2016).

On 16 August 2007, the remarkable EHT event, hereafter EHT07, occurred at Kumagaya. For EHT07, Takane and Kusaka (2011) found that the temperature increase was largely due to diabatic heating with subgrid-scale turbulent diffusion and sensible heat flux from the ground. This is similar to type-c foehn, hereafter called the "modified type-c foehn". The modified type-c foehn differs in two points from the type-c foehn. The type-c foehn is potential-flow accompanied with indirect heating due to the mechanical mixing (entrainment) whereas the modified type-c foehn is the isentropic drawdown accompanied with direct heating due to sensible heat flux from mountain surface.

On 23 July 2018, an EHT event occurred in the inland Kanto Plain at Kumagaya that had the highest maximum temperature ever recorded in Japan (41.1°C). However, the role of the foehn wind on the event has not yet been investigated. The purpose of this study is to quantify the effects of the foehn wind on this EHT event.

2. Data and numerical model

For the EHT events, we used observational data from the automated meteorological data acquisition system (AMeDAS) surface observation dataset (surface temperature, relative humidity, wind, and precipitation) and sounding data at Wajima (W in Fig. 1a) from the Japan Meteorological Agency (JMA). We also used radar data provided by JMA to check the precipitation in the windward region of the mountain. For the numerical model, we ran high-resolution simulations using the weather research and forecasting (WRF) model, version 3.9.1 (Skamarock et al. 2008).

The model configuration involved a multi-nested model as shown in Fig. S1 (see Supplement). The first domain consisted of 133 × 133 grid points in the x and y directions with a horizontal grid spacing of 6.0 km. The second domain consisted of 250 × 250 grid points with a horizontal grid spacing of 2.0 km. Both domains had 58 vertical sigma levels and a model top pressure of 100 hPa. The initial and boundary conditions were specified based on analysis of the Global-Spectrum-Model dataset from JMA. This dataset has a 0.5° × 0.5° horizontal grid spacing and a 6-hour temporal resolution. The model configurations are summarized in Table S1 (see Supplement).

Corresponding author: Hiroyuki Kusaka, University of Tsukuba, 1-1-1 Tennodai, Tsukuba, Ibaraki 302-8577, Japan. E-mail: kusaka@ccs.tsukuba.ac.jp.

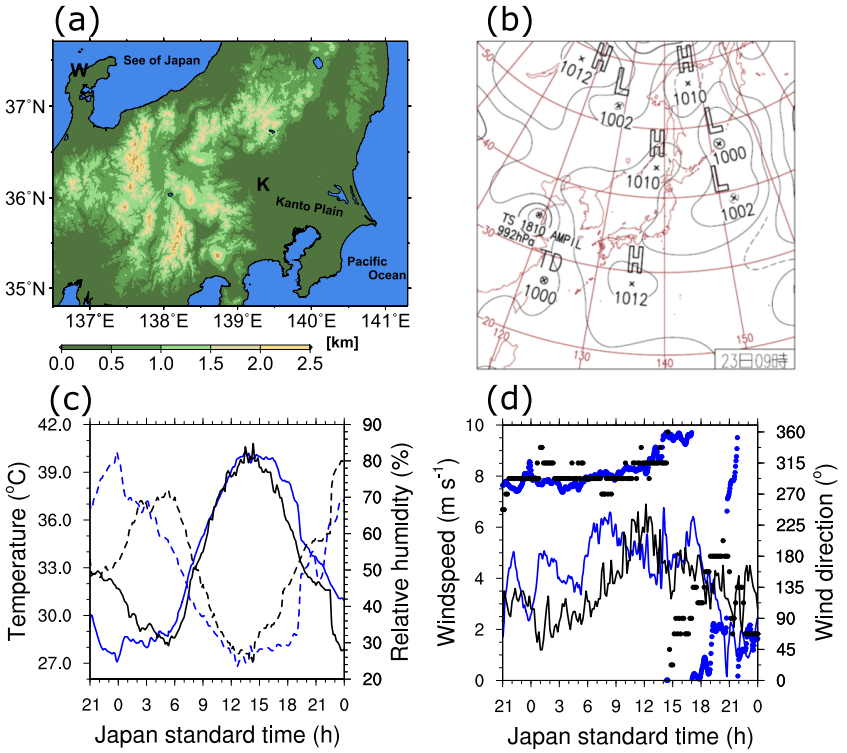

Fig. 1. Meteorological variables during the event. (a) Terrain around Kanto plain. Shadings show the terrain height with interval 0.5 km. "K" and "W" are the location of Kumagaya and Wajima, respectively. (b) Synoptic pressure pattern at 0900 JST on 23 July 2018 adapted from JMA (2018). (c) Time series of temperature (solid lines) and relative humidity (dashed) from 2100 JST on 22 July through 0000 JST on 24 July. Black curves are observations, blue are from the WRF model. (d) Same as (c) except for windspeed (solid lines) and wind direction (dots).

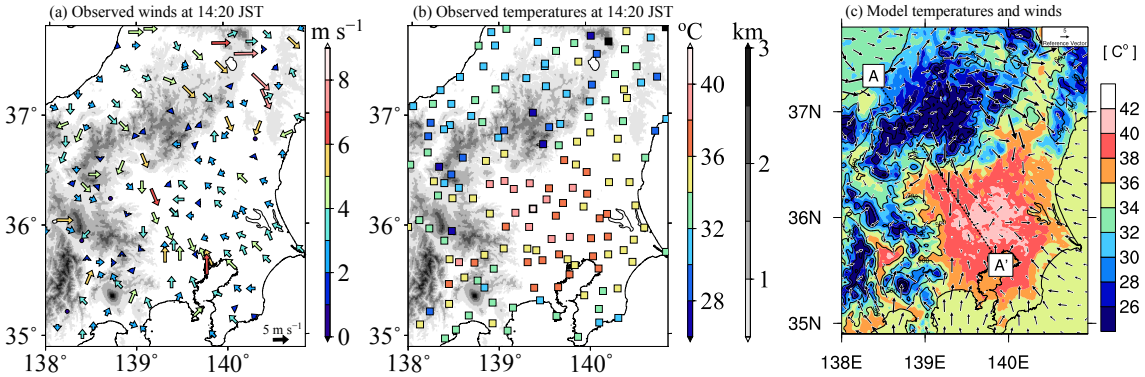

Fig. 2. Surface distributions at 1420 JST on 23 July 2018. (a) Observed surface wind. Vector color and length show the windspeed. Bold edged vector shows wind vector at Kumagaya. (b) Observed surface temperature. Bold edged square shows temperature at Kumagaya. Gray-scale shading shows the terrain height. (c) Calculated distributions of surface wind (vector) and surface temperature (color shading) from the WRF model. Contours show the terrain height with interval 0.25 km. Dashed line segment AA' is the location of the cross-section for Fig. 4.

3. Results and discussion

3.1 Observation data analysis

On 23 July 2018, the synoptic pressure pattern resembles a whale-tail pressure pattern (Fig. 1b). Moreover, for the six prior days, no precipitation fell at Kumagaya. These are all conditions for a remarkable EHT day (Takane et al. 2014).

At Kumagaya, the temperature is 28.6°C near sunrise (Fig. 1c, black solid curve). The temperature starts to rise at 0500 JST (Japan Standard Time), later reaching 41.1°C at 1423 JST, which is the highest ever recorded temperature in Japan. At the same time, northwesterly winds blow from the mountains to the plain around Kumagaya (Fig. 1d). The region of northerly winds coincides with the region of surface temperature ≥ 38.0°C (Figs. 2a and 2b). In addition, relative humidity at 1423 JST is less than 30% despite the summer (wet) season in Japan (Fig. 1c, black dashed curve). These features (winds from mountains, high-temperature, and low-humidity) are similar to those of foehn winds.

Southerly winds (i.e., sea breeze) blow in around the coastline of the Tokyo bay (Fig. 2a). The sea breezes start to blow along the coastline of the Pacific Ocean around 1000 JST (not shown) and reach at Kumagaya after 1700 JST (Fig. 1d). Thus, the sea breezes are delayed reaching the northwestern of Kanto plain because the sea breezes are obstructed by the northerly winds. These results suggest that the northerly winds have not only the direct effect to form the EHT event, but also indirect effects. Here, the indirect effects mean the preventing the cold advection from the ocean.

The type-b foehn wind involves precipitation on the windward of the mountains. But upon our examination of the precipitation, we found none in the windward region up to 12 hours before the highest temperature observed at Kumagaya (not shown). Thus, the EHT event does not rely on type-b foehn winds.

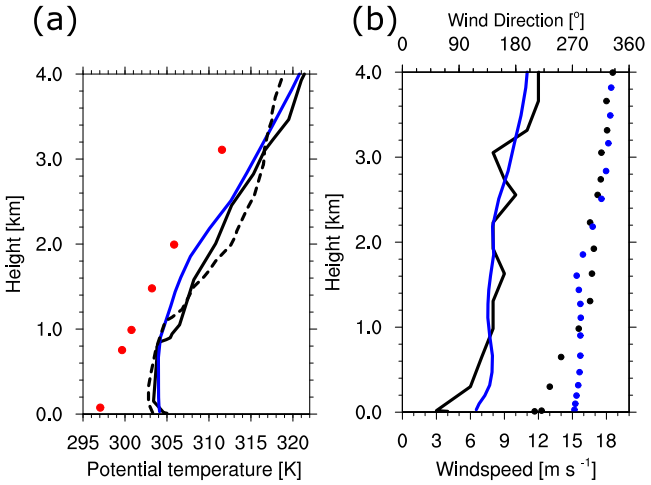

Fig. 3. Vertical profiles at Wajima at 0900 JST on 23 July 2018. (a) Potential temperature. Black solid lines show the radiosonde observations, blue shows model results. Dashed line shows the radiosonde observation in the EHT07 event at 0900 JST on 16 August 2007. Red circles show the 30-year average potential temperature (1981−2010). (b) Same as (a) except for windspeed. Circles show wind direction.

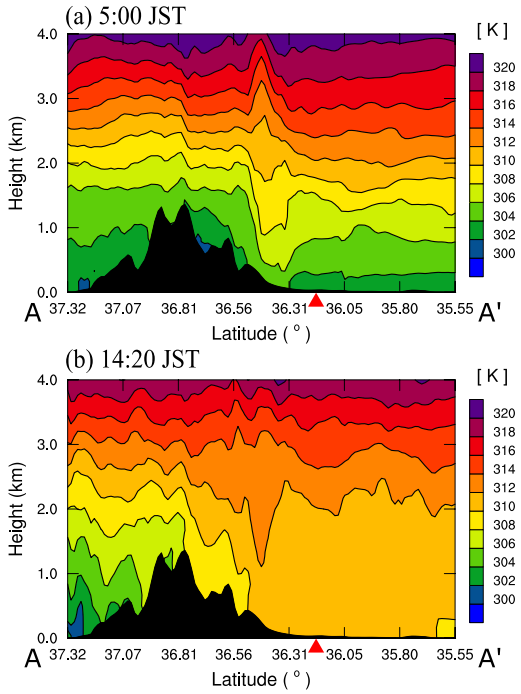

Fig. 4. Potential temperature along the AA' cross-section (see Fig. 3c) on 23 July 2018. (a) At 0500 JST. (b) At 1420 JST. Black area is the terrain. Red triangle shows the location of Kumagaya.

How about the type-a foehn wind? This type involves adiabatic heating in which air of high potential temperature (θ) descends from an upper layer, producing high temperatures in the leeward region of the mountains. In the windward region (Wajima) at 0900 JST on 23 July 2018, we find that θ values at up to 3.11 km (700 hPa) are about 5 K higher than the 30-year average between 1981 and 2010 (Fig. 3). We find a similar trend for the EHT07 event at 0900 JST on 16 August 2007. These results suggest that the EHT event is affected by the type-a foehn or type-c foehn, or the modified type-c foehn.

3.2 Results of the numerical experiment

We examine the model results to reveal what types of foehn wind blow in this EHT events. The WRF reproduces temporal change of temperature from 0600 to 1500 JST (Fig. 1c). In contrast, the WRF overestimate the temperature of 1.0°C in the afternoon because the simulated wind direction starts to change from northerly to southerly in the afternoon later than the observation (Fig. 1d). The WRF also reproduces the essential features of the spatial distribution of surface wind and temperature, except for the overestimation of the temperature in the southeastern Kanto plain (Fig. 2c). In addition, the WRF reproduces the vertical profiles of wind and potential temperature at Wajima well, except for the subsidence inversion (Fig. 3). It is considered that the subsidence inversion is not so important in the foehn flows because windspeed in this EHT events is weak. Therefore, the discrepancy does not probably influence foehn flow.

Now, in order to investigate the vertical structure of flows and its variation, we examine the simulated potential temperature along the cross-section AA' of Fig. 2c. At 0500 JST on 23 July, Fig. 4a shows that the contours of θ = 302~306 K lie between 1.0 and 2.0 km height in the windward region (37.32°N~36.56°N). These contours rapidly descend at the leeward plain of mountains (36.56°N~36.31°N), thereafter lying below about 1.0 km height in the leeward region. This lowering of the θ contour is an important feature of type-a foehn winds.

Later in the day, Fig. 4b shows that θ becomes remarkably high up to the 2.0 km height over the leeward slope of the mountain (southward of 36.81°N). Specifically, a near-neutral layer the height of which is about 2.0 km appears in the leeward region of the mountains (southward of 36.31°N). Because these changes appear near the surface during midday, the surface sensible heat flux is likely another important factor in the high temperature at Kumagaya.

3.3 Back-trajectory analysis and Lagrangian energy-budget analysis

The results of the numerical experiment suggest that both the type-a foehn winds and the surface sensible heat flux are important in the EHT event. Now, we quantitatively examine the heating effect of both factors using back-trajectory analysis and Lagrangian energy-budget analysis.

In the back-trajectory analysis, trajectories of 121 air parcels were released from the surface level of the model grid in a square area of 484 km^2 around Kumagaya at about the same time when the highest maximum temperature is observed (1421 JST 23 July 2018). The air parcels are tracked back from 1421 to 0400 JST using the wind fields at 3 min intervals which are simulated by the WRF model. In this EHT event, windspeed is small (< 8.0 m s^{-1}). In addition, high-temporal resolution dataset of winds (3 min interval) is used in this analysis. In such situation, truncation error of the trajectory is small (Seibert 1993), thus the air parcel trajectories have accuracy.

For the Lagrangian energy-budget analysis, we calculate the geopotential energy, the sensible heat energy and the dry static energy to determine which kind of wind blows along each parcel. The dry static energy (s) is composed of the geopotential energy (gz) and the sensible heat energy (C_pT):

$$s = gz + C_pT. \quad (1)$$

In Eq. (1), g is gravitational acceleration (m s^{-2}), C_p is specific heat at constant pressure (J kg^{-1} K^{-1}), and T is temperature (K). The dry static energy is a conserved quantity under any static, adiabatic process. Thus, if diabatic heating occurs under a small change of kinematic energy, then s increases; conversely if diabatic cooling occurs, then s decreases. Generally, diabatic heating is produced by water-vapor condensation, vapor deposition, freezing of liquid water, sensible heat flux from the ground, subgrid-scale turbulent diffusion, and radiation. In the present analysis, direct heating by radiation is small along the averaged trajectory because shortwave radiation can transmit the cloud-free atmosphere. Water-vapor condensation, vapor deposition, and freezing of liquid water are also small along the averaged trajectory because there is no

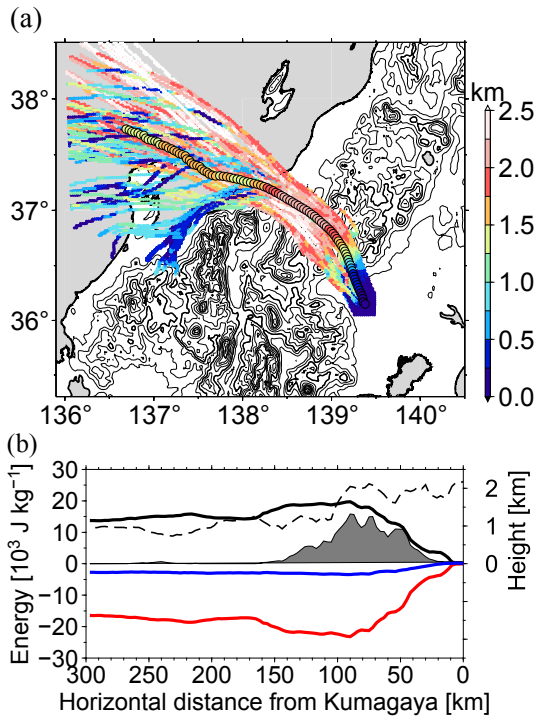

Fig. 5. Back-trajectories from the Kumagaya vicinity at 1421 JST 23 July 2018. (a) Parcel positions. The color indicates parcel height. Small circles show the trajectory of each parcel. Large circles with black perimeter show the ensemble-averaged trajectory of 121 air parcels. Solid gray contours are terrain height with 0.2 km intervals, the bold contours have a 1.0 km interval. (b) Energy terms (left axis) and mixed-layer height (right axis) along the ensemble averaged trajectories of air parcels shown in Fig. 5a. The black curve is the geopotential energy (gz), the red curve is the sensible heat energy (C_pT), the blue curve is the dry static energy (s), the dashed curve is the mixed-layer height, and gray shading is the terrain along the ensemble averaged trajectory of air parcels.

precipitation in the windward region of mountains. Therefore, the diabatic heating we consider here is (1) direct heating associated with surface sensible heat flux (DH) and (2) heating associated with the mixing by turbulent diffusion (MIX).

According to the back-trajectory analysis, the air parcels at the surface near Kumagaya at 1421 JST came from heights of 3.0 km or less over the Sea of Japan (Fig. 5a). The trajectory of 121 air parcels have large horizontal and vertical variances: the parcels originated from northward (southward) of 37.5°N tends to come from heights of 1.0 km or more (or less).

Figure 5b shows the Lagrangian mean energy budget along the ensemble-averaged trajectory of 121 air parcels. The geopotential energy (black curve) is about 14×10^3 J kg^{-1} and does not change much when the horizontal distance from Kumagaya (HDK) is between 100 and 300 km. At HDK = 100 km, the geopotential energy starts to decrease during the descent of the air parcel, and is about 0 J kg^{-1} at Kumagaya (HDK = 0 km). Therefore, the air parcel gains heat energy associated with adiabatic process. As the geopotential energy decreases, the sensible heat energy (red curve) increases. The sensible heat energy associated with the descent of the air parcel is about 16×10^3 J kg^{-1}. At HDK = 100 km, the air parcel penetrates the mixed boundary layer, and then the dry static energy (blue curve) starts to increase at HDK = 70 km. The dry static energy has increased by about 2.0×10^3 J kg^{-1} when the air parcel reaches Kumagaya. This diabatic heating is caused by DH and MIX because the dry static energy increases after penetration of the averaged air parcel in the mixed layer. Therefore, adiabatic heating accounts for about 87.5% (= $(14 \times 10^3$ J kg$^{-1})/(16 \times 10^3$ J kg$^{-1}) \times 100$) of the increase in the thermal energy gained by the averaged air parcel. The other 12.5% (= $(2.0 \times 10^3$ J kg$^{-1})/(16 \times 10^3$ J kg$^{-1}) \times 100$) is diabatic heating. If these energies are divided by C_p (1004 J kg^{-1} K^{-1}), the temperature increases of averaged air parcel by each factor are obtained. The increase by the adiabatic heating, by the diabatic heating, and the total increase are 14 K, 2 K, and 16 K, respectively.

These results show that the adiabatic heating (type-a foehn) dominates the EHT event. However, diabatic heating caused by DH and MIX was also crucial for the EHT event to reach the highest temperature in Japan (41.1°C).

These results are similar to the heat-budget of the air parcel in the mixed layer in the EHT07 event called "modified type-c foehn wind" (Takane and Kusaka 2011). Thus, this study finds that the mechanism of modified type-c foehn wind plays an important role, not only for the EHT07 event, but also on the EHT event on 23 July 2018.

In the EHT07 event, the parcels have two different courses and differ in the evolution of the heat budget (Takane and Kusaka 2011). In the EHT event studied here, the parcels have large horizontal and vertical variation in the windward region (Fig 5a), but the features of the heat budget do not vary strongly between individual parcels (not shown).

4. Conclusion

We used observational data and a numerical simulation to examine the effects of foehn winds on the record-breaking, all-time high temperature for Japan on 23 July 2018. In this event, the temperature reached 41.1°C at Kumagaya. Our main results are the following:

- This day satisfied four conditions for a likely remarkable EHT day (Takane et al. 2014). In particular, the synoptic pressure pattern had the "whale-tail" pressure pattern. Kumagaya had no precipitation for the 6 days prior to the event. From early morning, northerly winds blew down from the mountains to the plain around Kumagaya. And in the windward region, the potential temperatures up to 3.0 km elevation were about 5 K higher than those in the normal July.
- The northerly winds continued to blow until the highest temperature occurred. Moreover, the region of northerly winds coincided with the region having surface temperatures above 38.0°C.
- No precipitation occurred in the windward region of the mountains for the 12 hours before the event. In this windward region, the potential temperature up to 3.0 km was about 5 K higher than the 30-year average (1981−2010).
- According to back trajectory analysis, air parcels released at the surface on the time when the highest maximum temperature is observed at Kumagaya came from the region up to 3.0 km above sea level over the Sea of Japan.
- Lagrangian energy budget analysis shows that adiabatic heating accounts for about 87.5% of the increase in the thermal energy transfer to the air parcels, the rest being diabatic. The diabatic heating is caused by direct heating associated with surface sensible heat flux and heating associated with the mixing by turbulent diffusion. This mechanism is similar to the modified type-c foehn winds described in Takane et al. (2011). We conclude that modified type-c foehn wind occurs and play important role in the record-breaking high temperature on 23 July 2018.

Acknowledgments

This work was supported by Cabinet Office, Government of Japan, Cross-ministerial Strategic Innovation Promotion Program (SIP), "Technologies for creating next-generation agriculture, forestry and fisheries" (funding agency: Bio-oriented Technology Research Advancement Institution, NARO). We used Generic Mapping Tool and NCAR Command Language to draw figures in the present study.

Edited by: R. Kawamura

Supplement

Supplementary Fig. S1 shows the model domains and terrains. Supplementary Table S1 shows the configuration of the numerical experiments.

References

Arakawa, S., 1969: Climatological and dynamical studies on the local strong winds, mainly in Hokkaido, Japan. *Geophys. Mag*, **34**, 349−425.

Brinkmann, W. A. R., 1971: What is a foehn? *Weather*, **26**, 230−240, doi:10.1002/j.1477-8696.1971.tb04200.x.

Brinkmann, W. A. R., 1973: A climatological study of strong downslope winds in the Boulder area. *NCAR Cooperative Thesis 27/INSTARR Occasional Paper 7*, University of Colorado, 229 pp.

Brinkmann, W. A. R., 1974: Strong downslope winds at Boulder, Colorado. *Mon. Wea. Rev.*, **102**, 592−602.

Chen, F., and J. Dudhia, 2001: Coupling an advanced land-surface/hydrology model with the Penn State/NCAR MM5 modeling system. Part I: Model description and implementation. *Mon. Wea. Rev.*, **129**, 569−585.

Dudhia, J., 1989: Numerical study of convection observed during the winter monsoon experiment using a mesoscale two-dimensional model. *J. Atmos. Sci.*, **46**, 3077−3107.

Elvidge, A. D., and I. A. Renfrew, 2016: The Causes of foehn warming in the lee of mountains. *Bull. Amer. Meteor. Soc.*, **97**, 455−466, doi:10.1175/BAMS-D-14-00194.1.

Ficker, H. V., 1910: Innsbrucker Föhn-studien IV. Weitere Beiträge zur Dynamik des Föhns. *Denkschr. Kaiserl. Akad. d. Wiss., Math. Natwiss. Kl.*, **85**, 114−173.

Fujibe, F., 1995: Temperature rising trends at Japanese cities during the last hundred years and their relationships with population, population increasing rates and daily temperature ranges. *Pap. Meteor. Geophys.*, **46**, 35−55.

Hann, J., 1866: Zur Frageüber den Ursprung des Föhn. *Z. Österr. Ges. Meteorol.*, **1**, 257−263.

Hann J., 1867: Der Föhn in denösterreichischen Alpen. *Z. Österr. Ges. Meteorol.*, **2**, 433−445.

Hoinka, K. P., 1985: What is a foehn clearance? *Bull. Amer. Meteor. Soc.*, **66**, 1123−1132, doi:10.1175/1520-0477(1985)066<1123:WIAFC>2.0.CO;2.

Hong, S. Y., J. Dudhia, and S. H. Chen, 2004: A revised approach to ice microphysical processes for the bulk parameterization of clouds and precipitation. *Mon. Wea. Rev.*, **132**, 103−120.

Ikawa, M., and Y. Nagasawa, 1989: A numerical study of a dynamically induced foehn observed in the Abashiri-Ohmu area. *J. Meteor. Soc. Japan*, **67**, 429−458.

Janjic, Z. I., 1994: The Step–Mountain Eta Coordinate Model: Further developments of the convection, viscous sublayer, and turbulence closure schemes. *Mon. Wea. Rev.*, **122**, 927−945, doi:10.1175/1520-0493(1994)122%3c0927:TSMECM%3e2.0.CO;2.

JMA, 2018: Daily weather chart in July 2018 (in Japanese) (Available online at https://www.data.jma.go.jp/fcd/yoho/data/hibiten/2018/201807.pdf, accessed 22 September 2018).

Kusaka, K., H. Kondo, Y. Kikegawa, and F. Kimura, 2001: A simple single-layer urban canopy model for atmospheric models: Comparison with multi-layer and slab models. *Bound.-Layer Meteor.*, **101**, 329−358.

Kain, J. S., 2004: The Kain–Fritsch convective parameterization: An update. *J. Appl. Meteor.*, **43**, 170−181.

Kusaka, H., and F. Kimura, 2004a: Coupling a single-layer urban canopy model with a simple atmospheric model: Impact on urban heat island simulation for an idealized case. *J. Meteor. Soc. Japan*, **82**, 67−80.

Kusaka, H., and F. Kimura, 2004b: Thermal effects of urban canyon structure on the nocturnal heat island: Numerical experiment using a mesoscale model coupled with an urban canopy model. *J. Appl. Meteor.*, **43**, 1899−1910.

Miltenberger, A. K., S. Reynolds, and M. Sprenger., 2016: Revisiting the latent heating contribution to foehn warming: Lagrangian analysis of two foehn events over the Swiss Alps. *Quart. J. Roy. Meteor. Soc.*, **142**, 2194−2204, doi:10.1002/qj.2816.

Mlawer, E. J., S. J. Taubman, P. D. Brown, M. J. Iacono, and S. A. Clough, 1997: Radiative transfer for inhomogeneous atmospheres: RRTM, a validated correlated–k model for the longwave. *J. Geophys. Res.*, **102**, 16663−16682.

Ólafsson, H., 2005: The heat source of the foehn. *Hrvat. Meteor. Časopis*, **40**, 542−545.

Richner, H., and P. Hächler, 2013: Understanding and forecasting Alpine foehn. *Mountain Weather Research and Forecasting: Recent Progress and Current Challenges*, F. K. Chow, S. F. J. De Wekker, and B. J. Snyder, Eds., Germany, Springer, 219−260.

Scorer, R. S., 1978: *Environmental Aerodynamics*. Vol. 815. Ellis Horwood, 488 pp.

Scorer, R. S., and H. Klieforth, 1959: Theory of mountain waves of large amplitude. *Quart. J. Roy. Meteor. Soc.*, **85**, 131−143.

Skamarock, W. C., J. B. Klemp, J. Dudhia, D. O. Gill, D. M. Barker, M. G. Duda, X. Huang, W. Wang, and J. G. Powers, 2008: A description of the Advanced Research WRF Version 3. NCAR Tech. Note, NCAR/TN-475+STR, 126 pp.

Seibert, P., 1990: South foehn studies since the ALPEX experiment. *Meteor. Atmos. Phys.*, **43**, 91−103.

Seibert, P., 1993: Convergence and accuracy of numerical methods for trajectory calculation. *J. Appl. Meteor.*, **32**, 558−566.

Takane, Y., and H. Kusaka, 2011: Formation mechanisms of the extreme high surface air temperature of 40.9°C observed in the Tokyo metropolitan are Considerations of dynamic foehn and foehnlike wind. *J. Appl. Meteor. Climatol.*, **50**, 1827−1841, doi:10.1175/JAMC-D-10-05032.1.

Takane, Y., H. Kusaka, and H. Kondo, 2014: Climatological study on mesoscale extreme high temperature events in inland of the Tokyo metropolitan area, Japan, during the past 22 years. *Int. J. Climatol.*, **34**, 3926−3938, doi:10.1002/joc.3951.

Takane, Y., H. Kusaka, and H. Kondo, 2015: Investigation of a recent extreme high-temperature event in the Tokyo metropolitan area using numerical simulations: The potential role of a 'hybrid' foehn wind. *Quart. J. Roy. Meteor. Soc.*, **141**, 1857−1869, doi:10.1002/qj.2490.

Whiteman, C. D., 2000: *Mountain Meteorology: Fundamentals and Applications*. Oxford University Press, 355 pp.

WMO, 1992: *International Meteorological Vocabulary (2nd edn)*, World Meteorological Organization, Geneva, Switzerland, WMO/OMM/BMO-No.182, 784 pp.

Manuscript received 22 October 2018, accepted 19 December 2018
SOLA: https://www.jstage.jst.go.jp/browse/sola/